EVALUATION OF A MONOSTATIC STAP RADAR RANGE-COMPENSATION METHOD APPLIED TO SELECTED BISTATIC CONFIGURATIONS

Fabian D. Lapierre and Jacques G. Verly

University of Liège, Department of Electrical Engineering and Computer science
Sart Tilman, Building B28, B-4000 Liège, Belgium
f.lapierre@ulg.ac.be, jacques.verly@ulg.ac.be

ABSTRACT

The detection of slow moving targets by a moving bistatic pulsed Doppler radar system is addressed. Optimum clutter rejection is achieved using space-time adaptive processing (STAP). This requires estimating the clutter-plus-noise covariance matrix using a sequence of snapshots at successive ranges. For most monostatic and for all bistatic radar configurations, these snapshots are range-dependant. The estimator is then biased and not accurate. A compensation method originally developped for the monostatic case is applied to selected bistatic configurations and its performance assessed in these new conditions.

1. INTRODUCTION

The detection of slow moving targets using a moving pulsed Doppler radar system is a problem of great interest. One distinguishes between monostatic (MS) configurations, where the radar transmitter and receiver are colocated and bistatic (BS) configurations, where they are physically separated. In either case, a train of coherent pulses is transmitted and the corresponding returns are sensed at each of the elements of a linear antenna array.

Optimum clutter rejection is achieved by using a collection of techniques known as space-time adaptive processing (STAP). While STAP research was initially developped for MS configurations [1, 2], it is now increasingly directed to BS configurations [3].

The adaptive weights used by STAP are computed using a clutter-plus-noise covariance matrix estimated from data collected at successive ranges. An accurate estimate of this matrix can be obtained only if the structure of the clutter spectrum remains unchanged over the range interval used for the estimation. The most significant feature of the clutter spectrum is a “clutter ridge” [1]. In the MS sidelooking (SL) configuration, where the antenna is aligned with the radar velocity vector, the position, shape and size of this ridge remain constant as the range changes. In all other MS configurations and in all BS configurations, the ridge appearance changes considerably with range. This is the so-called “range-dependence problem” in STAP.

Two approaches have been proposed so far to deal with this problem. The “Doppler-warping” method [4] works well in near-SL MS configurations. It has been applied to BS configurations but the reported performance is poor [5]. The scaling method [6] was initially developped for arbitrary MS configurations, where it works fairly well. The goal of the present paper is to test the same method on selected BS configurations.

2. BISTATIC GEOMETRY

Figure 1 shows a typical bistatic geometry, which consists of a transmitter, a receiver and a scatterer, respectively located at T, R and S. The transmitter and the receiver are typically mounted on their own separate platforms, either airborne or spaceborne. The scatterer can be a target or an elementary clutter region.

The origin of the coordinate system (x, y, z) is choosen to coincide with T. Its orientation is such that the x-axis points in the same direction as the transmitter velocity vector $\underline{\boldsymbol{v}}_T$ and that the z-axis points vertically up. The receiver velocity vector $\underline{\boldsymbol{v}}_R$ is assumed to be located in a horizontal plane and to make an angle α_R with respect to the x-axis. Clearly, we assume $\alpha_T = 0$.

The receiver antenna is linear. It is assumed to be located in a horizontal plane and to make an angle δ with respect to the x-axis. The angular positions of S measured from the antenna axis, $\underline{\boldsymbol{v}}_T$ and $\underline{\boldsymbol{v}}_R$ are respectively given by the “cone” angles ξ, ξ_d^T and ξ_d^R. The bistatic range R_b is the distance from T to S to R.

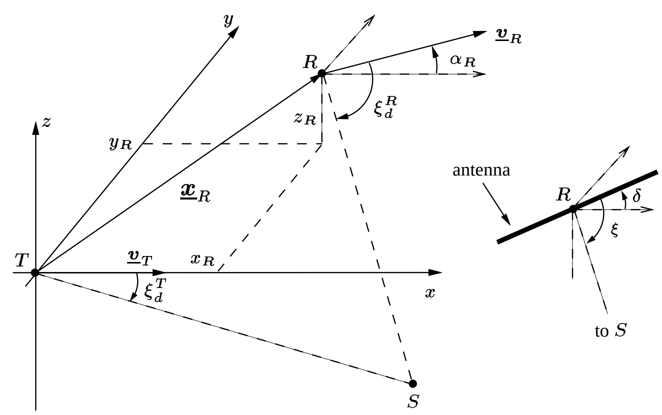

Figure 1: Elements of a BS radar configuration.

3. DIRECTION-DOPPLER CURVES

In the present case, the radar system is expected to determine at least three basic parameters for each scatterer of interest : the angular position ξ, the BS range R_b and the relative velocity v_r (measured with respect to the receiver). The related parameters that are more directly measured from the radar returns are the spatial frequency f_s [2]

$$f_s = \lambda_c^{-1} \cos \xi,$$

where λ_c is the wavelength, the round-trip delay $\tau_b = R_b/c$ (c is the speed of the light) and the Doppler frequency f_d, which, for a stationnary scatterer (such as a clutter patch) is [2]

$$f_d = \lambda_c^{-1} v_T \cos\xi_d^T + \lambda_c^{-1} v_R \cos\xi_d^R.$$

The parameters ξ, R_b and v_r can easily be computed from the parameters f_s, τ_b and f_d.

For any given BS configuration and for any given R_b, all stationnary scatterers at the selected R_b map onto a curve showing the relation that exists between f_s and f_d for any such scatterer. Each subfigure in Fig. 2 corresponds to a different BS configuration and each curve within each subfigure to a different R_b. Each curve is called a "direction-Doppler (DD)" curve. It is implicitely parameterized by the position of each scatterer in a horizontal plane at some specified height and at the R_b of interest.

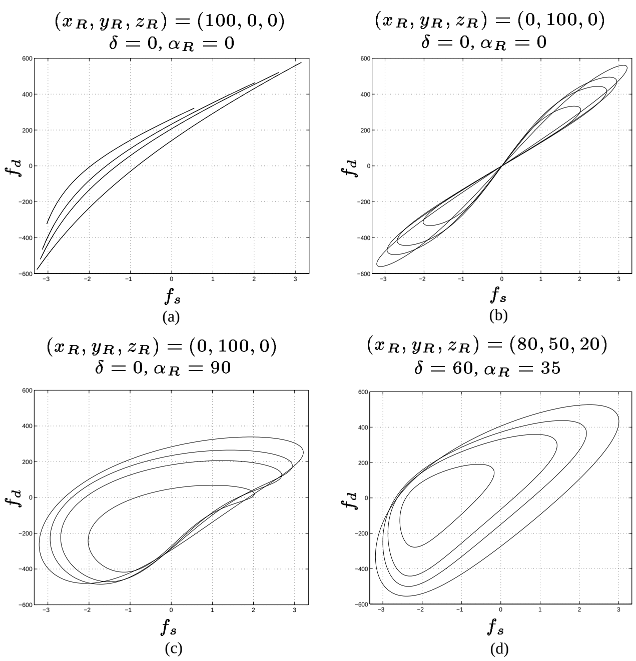

Figure 2: Examples of DD curves for different BS configurations (with parameters given above) and BS ranges R_b (of 170, 210, 250 and 400 km).

The plots of Fig. 2 show that the relationship between f_s and f_d vary significantly, not only from one BS configuration to another (as in the MS case), but also from one range to another (in contrast to the MS SL case). Finally, one can show that there is a direct relation between the DD curve and the "clutter ridge" observed in the clutter spectrum discussed below.

4. OPTIMUM STAP PROCESSOR

A train of M coherent pulses is transmitted, the returns are sensed at each of the N antenna-array elements, and the sensed returns are sampled at a number of discrete ranges covering the range interval of interest. The signal samples are thus equispaced in time, space and range. The result is a sequence of $M \times N$ data arrays at successive ranges. Each such array is called a "snapshot".

It can be shown that the $M \times N$ snapshot corresponding to a single scatterer (target or clutter patch) with normalized spatial and Doppler frequencies $\nu_s = (\lambda_c/2)\, f_s$ and $\nu_d = (\lambda_c/(v_R + v_T)) f_d$ (where $v_R = |\underline{\boldsymbol{v}}_R|$ and $v_T = |\underline{\boldsymbol{v}}_T|$) and with range R_b can be written as a $MN \times 1$ vector [2]

$$\underline{\boldsymbol{y}}(\nu_s, \nu_d) = \beta_r \underline{\boldsymbol{v}}(\nu_s, \nu_d),$$

where β_r comes from the radar equation and $\underline{\boldsymbol{v}}(\nu_s, \nu_d)$ is the $MN \times 1$ steering vector

$$\underline{\boldsymbol{v}}(\nu_s, \nu_d) = \underline{\boldsymbol{b}}(\nu_d) \otimes \underline{\boldsymbol{a}}(\nu_s), \tag{1}$$

where $\otimes$ is the Kronecker product and $\underline{\boldsymbol{a}}(\nu_s)$ and $\underline{\boldsymbol{b}}(\nu_d)$ are the $N \times 1$ spatial and $M \times 1$ temporal steering vectors given by

$$\underline{\boldsymbol{a}}(\nu_s) = (1 \ldots e^{j2\pi\nu_s n} \ldots e^{j2\pi\nu_s(N-1)})^T \tag{2}$$

$$\underline{\boldsymbol{b}}(\nu_d) = (1 \ldots e^{j2\pi\nu_d m} \ldots e^{j2\pi\nu_d(M-1)})^T. \tag{3}$$

The clutter snapshot $\underline{\boldsymbol{y}}_c(\nu_s, \nu_d)$ is found by integrating $\underline{\boldsymbol{y}}(\nu_s, \nu_d)$ over the isorange curve defined by the intersection of the isorange ellipsoid with the ground and parameterized by some angle ϕ, which is the angle running along the curves of Fig. 2. One has

$$\underline{\boldsymbol{y}}_c(\nu_s, \nu_d) = \int_0^{2\pi} \beta_c(\phi)\, \underline{\boldsymbol{v}}(\nu_s(\phi), \nu_d(\phi))\, d\phi.$$

In general, the power spectral density (PSD) of a stationnary discrete random process is the Fourier transform (FT) of its autocorrelation sequence. Since we do not generally have access to the full autocorrelation, we must use spectral estimation methods.

The simplest approach in the case of clutter is to take the 2D discrete space-time FT of the $MN \times MN$ correlation matrix

$$\underline{\underline{\boldsymbol{Q}}}_c = E\{\underline{\boldsymbol{y}}_c\, \underline{\boldsymbol{y}}_c^\dagger\}.$$

This gives a poor-resolution estimate of the clutter PSD. Among other approaches, the minimum variance estimator (MVE) works particularly well in STAP [1]. Clutter PSDs computed with either method shows a concentration of energy along a particular "curve" in the array representing the PSD. The support of this "clutter ridge" is in direct correspondence with the related DD curve in the continuous (f_s, f_d)-plane.

The STAP weights providing optimum clutter rejection are given by the $MN \times 1$ vector [7]

$$\underline{\boldsymbol{w}}_{\text{opt}}(\nu_s, \nu_d) = \underline{\underline{\boldsymbol{Q}}}^{-1} \underline{\boldsymbol{v}}(\nu_s, \nu_d), \tag{4}$$

where $\underline{\underline{\boldsymbol{Q}}}$ is the sum of the covariance matrices $\underline{\underline{\boldsymbol{Q}}}_c$ for the clutter and $\underline{\underline{\boldsymbol{Q}}}_n = \underline{\underline{\boldsymbol{I}}}$ for a noise assumed to be spatially and temporally white (Jammers could also be considered). Since $\underline{\underline{\boldsymbol{Q}}}_c$ generally varies with R_b, $\underline{\underline{\boldsymbol{Q}}}_c$ must be estimated for each R_b and the optimum weights must also be computed for each R_b. We assume that successive discrete ranges are indexed with the integer r. At each r, $\underline{\underline{\boldsymbol{Q}}}$ is ideally estimated using the $(N_r - 1)/2$ snapshots on either side of r, i.e.,

$$\widehat{\underline{\underline{\boldsymbol{Q}}}}(r) = \frac{1}{N_r} \sum_{k \in K_r} \underline{\underline{\boldsymbol{Q}}}(k), \qquad \underline{\underline{\boldsymbol{Q}}}(k) = \underline{\boldsymbol{y}}(k) \underline{\boldsymbol{y}}^\dagger(k), \tag{5}$$

where K_r is the appropriate set of indices and $\underline{\boldsymbol{y}}(k)$ the received snapshot $\underline{\boldsymbol{y}}$ corresponding to range k. An unbiased estimator can be obtained if the clutter ridge is range-independant. However, this happens only for MS SL configurations.

The performance of a processor using arbitrary weights $\underline{\boldsymbol{w}}$ is measured by the signal-to-interference-plus-noise (SINR) loss

$$\mathrm{L_{SINR}} = \frac{\mathrm{SINR}}{\mathrm{SINR_0}} = \frac{\left|\underline{\boldsymbol{w}}^\dagger \underline{\boldsymbol{v}}\right|^2}{(\underline{\boldsymbol{w}}^\dagger \underline{\underline{\boldsymbol{Q}}}\,\underline{\boldsymbol{w}})(\underline{\boldsymbol{v}}^\dagger \underline{\boldsymbol{v}})},$$

where $\mathrm{SINR_0}$ is the SINR in the absence of interference (clutter). The values of $\mathrm{L_{SINR}}$ range from a minimum equal to the clutter-to-noise ratio to a maximum of one, indicating that the processor performance is not degraded by clutter. Optimum (theorical) performance is achieved with $\underline{\boldsymbol{w}} = \underline{\boldsymbol{w}}_{opt}$. In practice, the processor performance is degraded by the losses due to the estimation of $\underline{\underline{\boldsymbol{Q}}}$ and to the range dependence of the clutter ridge.

5. DOPPLER-WARPING METHOD

The Doppler-warping method was initially developped for near-SL MS configurations. It applies a linear transformation, described by a $MN \times MN$ matrix $\underline{\underline{\boldsymbol{T}}}(k)$, to each snapshot $\underline{\boldsymbol{y}}(k)$ [4]. The goal of $\underline{\underline{\boldsymbol{T}}}(k)$ is to apply a common Doppler shift Δ_{f_d} to all spatial frequencies f_s so as to bring the clutter ridge in registration for all ranges. Whereas the compensation is perfect at a particular f_s, it is approximate at any other f_s. Performance degrades as one moves away from the SL configuration in the MS case and is poor in the BS case [5].

6. SCALING METHOD

The scaling method was initially developped for all MS configurations [6]. It applies a transformation to each matrix $\underline{\underline{\boldsymbol{Q}}}(k) = \underline{\boldsymbol{y}}(k)\underline{\boldsymbol{y}}^\dagger(k)$ prior to its use in the calculation of $\widehat{\underline{\underline{\boldsymbol{Q}}}}$ in Eq. (5), this to bring into registration the kth clutter ridge onto the rth one.

First, we develop and test the transformation on the (continuous) DD curves. Then, we adapt it so it can be applied to the (discrete) matrix $\underline{\underline{\boldsymbol{Q}}}(k)$. It is important to understand that, in the first case, we develop the method in the space-time frequency domain, whereas, in the second, we adapt it to work directly in the space-time domain. Indeed, we do not have access to the true FT domain if we apply spectrum estimation methods!

We use $\mathcal{C}_r$ to denote the reference DD curve at r and $\mathcal{C}_k$ to denote curves at neighboring k's. We want to bring all $\mathcal{C}_k$'s into registration with $\mathcal{C}_r$. To do so, we first rename the original variables (f_s, f_d) for each curve as (f'_s, f'_d). All curves $\mathcal{C}_k$ are then transformed into the common system of coordinates (f_s, f_d), which is also that of $\mathcal{C}_r$. This is done by using a particular affine transformation $\underline{\underline{\boldsymbol{T}}}(k)$. Using homogeneous coordinates for convenience, we have

$$(f'_s\ f'_d\ 1)^T = \underline{\underline{\boldsymbol{T}}}(k)\,(f_s\ f_d\ 1)^T.$$

The particular affine transformation used corresponds to first bringing the "center" (defined here to be the center of the curve's bounding rectangle) of each $\mathcal{C}_k$ to the origin of its (f'_s, f'_d) axes, then scaling this translated curve, possibly inequally along f'_s and f'_d, and finally bringing the scaled curve to the "center" of $\mathcal{C}_r$. Thus, $\underline{\underline{\boldsymbol{T}}}(k)$ is of the form

$$\begin{pmatrix} 1 & 0 & \Delta^2_{f_s} \\ 0 & 1 & \Delta^2_{f_d} \\ 0 & 0 & 1 \end{pmatrix} \begin{pmatrix} S_{f_s} & 0 & 0 \\ 0 & S_{f_d} & 0 \\ 0 & 0 & 1 \end{pmatrix} \begin{pmatrix} 1 & 0 & \Delta^1_{f_s} \\ 0 & 1 & \Delta^1_{f_d} \\ 0 & 0 & 1 \end{pmatrix},$$

where $\Delta^i_{f_s}$ and $\Delta^i_{f_d}$ are the space and time offsets for the ith translation and S_{f_s} and S_{f_d} the space and time scaling factors.

Since the algorithm was initially developped for MS configurations, where all DD curves in a given range interval are exact scaled versions of each other, the algorithm was not expected to work perfectly in all BS cases. Figure 3 shows the result of applying the scaling method to the BS DD curves of Fig 2. Clearly, the more similar the original curves, as in Fig. 2(a) and (b), the better the results.

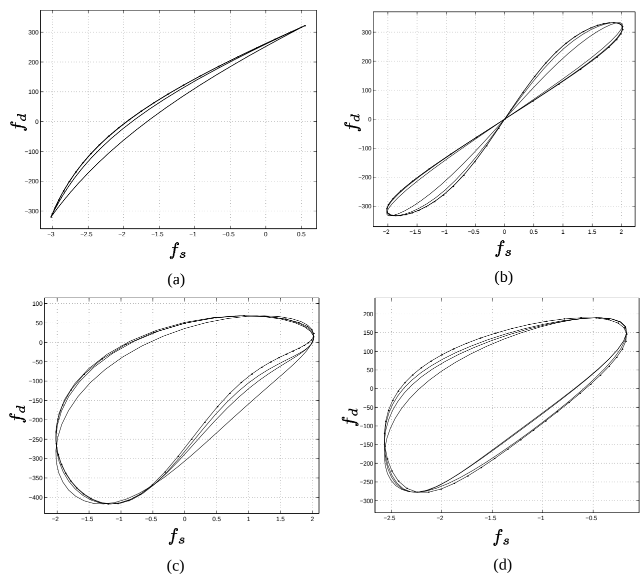

Figure 3: Result of application of the scaling method to the DD curves of Fig. 2. The dotted curve, which may be difficult to see, is the reference curve $\mathcal{C}_r$ corresponding to $R_b = 170$ km.

Since the clutter ridges of PSDs are the practical equivalent of the DD curves, it is tempting to apply the above method to them. In practice, however, we only have access to the matrices $\underline{\underline{\boldsymbol{Q}}}(k) = \underline{\boldsymbol{y}}(k)\underline{\boldsymbol{y}}^\dagger(k)$. The question is thus how to adapt the $\underline{\underline{\boldsymbol{Q}}}(k)$'s to achieve the desired registration of the clutter ridges. One of the problems is that the estimators, such as the MVE, provide a nonlinear relation between space-time and its spectral domain. It is thus not obvious how to express the particular spectral-domain affine transformation $\underline{\underline{\boldsymbol{T}}}(k)$ in the space-time domain of the $\underline{\underline{\boldsymbol{Q}}}(k)$'s. The procedure used is as follows.

Each $\underline{\underline{\boldsymbol{Q}}}(k)$ is regarded as a 2D sequence with finite support and is converted to a 2D continuous function by applying an interpolation filter to the elements of the sequence. The interpolation in the space-time domain corresponds to applying a window $W(U, V)$ in the Fourier or spectral domain. This window eliminates the periodic replicas of the central 2D "period" of the spectrum. If these replicas were not eliminated, they would move into the central "period" of the spectrum following a scaling operation corresponding to a contraction of the spectrum. The best results were obtained by using a 2D Kaiser window [8]

$$w(U, V) = w_1(U)w_2(V),$$

where

$$w_i(W) = \begin{cases} \frac{I_0\left[\beta\left\{1-(\frac{W}{W_f})^2\right\}^{1/2}\right]}{I_0(\beta)} & |W| \leq W_f \\ 0 & \text{otherwise,} \end{cases}$$

where $I_0(.)$ is the zeroth-order modified Bessel function of the first kind. W_f is the limit of the visible clutter spectrum on the U and V axes and is thus equal to 0.5 (for the two axes) for normalized frequencies. The best choice for β is found to be three.

The continuous 2D function obtained following interpolation is then subjected to the transformations corresponding to the translations and scaling that we want to achieve in the spectral domain. The transformatios that are needed are the phase shifts and scaling suggested by the following Fourier transform pairs

$$\begin{aligned} f(x,y)\, e^{j2\pi(u_0 x + v_0 y)} &\rightleftharpoons F(u-u_0, v-v_0) \\ f(\frac{x}{S_x}, \frac{y}{S_y}) &\rightleftharpoons S_x S_y\, F(S_x u,\, S_y v). \end{aligned}$$

The transformed 2D function is then resampled on a grid identical to that of the original matrix $\underline{\underline{\boldsymbol{Q}}}(k)$. The whole transformation described can be represented by some operator $S_k[.]$, so that

$$\underline{\underline{\boldsymbol{Q}}}_s(k) = S_k\left[\underline{\underline{\boldsymbol{Q}}}(k)\right].$$

Figure 4 illustrates the transformation of the power spectrum of a particular $\underline{\underline{\boldsymbol{Q}}}(k)$ following the application of the operator $S_k[.]$.

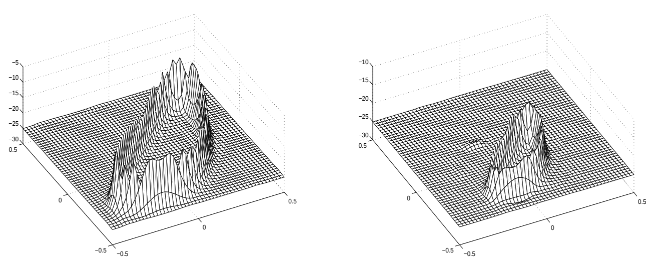

Figure 4: Power spectrum (a) before and (b) after scaling for configuration (d) in Fig. 2 and $\beta = 3$.

Finally, the estimate $\widehat{\underline{\underline{\boldsymbol{Q}}}}(r)$ of the desired covariance matrix $\underline{\underline{\boldsymbol{Q}}}$ for range r is

$$\widehat{\underline{\underline{\boldsymbol{Q}}}}(r) = \frac{1}{N_r}\sum_{k \in K_r} S_k\left[\underline{\underline{\boldsymbol{Q}}}(k)\right],$$

where $K_r = \{r+1, \ldots, r+N_r\}$. Note that we currently use the N_r ranges following r.

The performance of the scaling method is illustrated in Fig. 5. It is clear that the method leads to a reduction of the width of the clutter notch. However, a reduction of the depth of the notch is also observed. This appears to be a consequence of the use of the Kaiser window.

7. CONCLUSION

The rejection of clutter in bistatic STAP is a challenging problem. This is due to the range-dependence of the direction-Doppler curves and of the corresponding clutter ridges. The scaling method discussed here is a compensation method originally developped for monostatic STAP. This paper demonstrates that this method works well in many, but not all, bistatic configurations. The method relies on a particular form of the affine transformation. We are currently investigating the use of a general affine transformation and of other more general transformations.

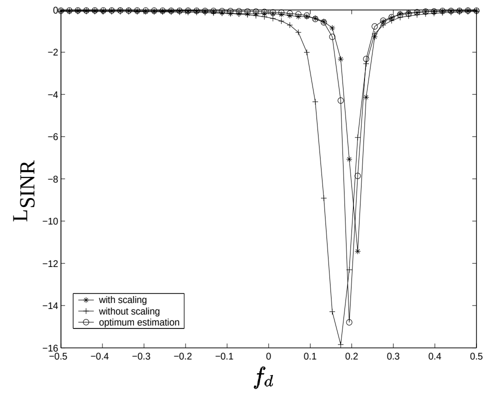

Figure 5: SINR losses for the configuration (a) of Fig. 2.

8. REFERENCES

[1] R. Klemm, *Space-Time Adaptive Processing : Principles and Applications*, IEE Radar, Sonar, Navigation and Avionics 9, 2000.

[2] J. Ward, *Space-time adaptive processing for airborne radar*, Technical Report 1015, Lincoln Laboratory MIT, 1994.

[3] R.L. Fante, *Ground and airborne target detection with bistatic adaptive space-based radar*, Proc. IEEE Radar Conference, 1999, pp 7-11.

[4] G.K. Borsari, *Mitigating effects on STAP processing caused by an inclined array*, IEEE National Radar Conference, Dallas, 1998, pp 135-140.

[5] S.M. Kogon and M.A. Zatman, *Bistatic STAP for Airborne Radar Systems*, ASAP Conference, MIT, Lincoln Laboratory, Boston, 2001.

[6] F.D. Lapierre and J.G. Verly, *The range-dependence problem of clutter spectrum for non-sidelooking monostatic STAP radars*, 21st Benelux Meeting on Systems and Control, Veldhoven, The Netherlands, 2002.

[7] L.E. Brennan and L.S. Reed, *Theory of Adaptive Radar* IEEE Transactions on Aerospace and Electronic Systems (AES), 1973, Vol 9, No 2, pp 237-252.

[8] A.V. Oppenheim and R.W. Schafer, *Discrete-Time Signal Processing*, Prentice Hall, 1999.